Chapter-3

Pr^{3+} doped Lead Tungsten Tellurite glasses for visible Red Lasers

Paper based on this chapter is published in Ceramics International, 40 (2014) 6261-6269.

3.1. Introduction

In quite recent years glasses doped with rare-earth doped glasses have fascinated several researchers because of their potential applications in the development of several optical devices like optical amplifiers, solid state lasers, laser wave guides, light converters, sensors, three dimensional displays, colour display devices, biomedical diagnostics and up conversion lasers [69-77]. The spectral characteristics of rare-earth ions are reliant on host glass composition, concentration of dopant ion and ambient temperatures [78]. Heavy metal oxide glasses are suitable candidates for the development of non-linear optical devices, electro-optic modulators, electro-optic switches, solid state laser materials and IR technologies because of their high density, refractive index and low phonon energy [79-82].

Pr^{3+} doped glasses with low phonon energy are used very much for compact solid state lasers emitting in visible region. Pr^{3+}ions in glasses have relatively good number of absorption bands in the vis-NIR regions due to which it has various technological applications as functional photonic materials like optical fibre amplifiers, lasers and wavelength converting devices. Pr^{3+} is a significant optical activator with its several meta-stable states that offers stimulated emissions in blue, green, orange, red and infrared regions [102]. In the present work, lead tungsten tellurite (LTT) glasses were prepared by varying Pr^{3+} concentration to study the optical and luminescent properties to identify the better glass for visible solid state laser devices.

3.2. Experimental

3.2.1 Glass Preparation

Lead tungsten tellurite glasses doped with different concentrations of Pr^{3+} ions were prepared by melt quenching technique. All chemical used to prepare the LTT glasses were analar grade with 99.9% purity. The glass composition of LTT glasses and their labeling are given in Table 3.1. All the reagents are thoroughly mixed in an agate mortar for 2 hrs to get uniform mixing and then melted using a silica crucible at 735^0C in a programmable furnace for about 25 min. The resultant melts were rotated 3 to 4 times before quenching to achieve homogenous mixture. Such melts were then poured on a preheated brass mould and pressed quickly with another brass plate. The samples were annealed in another furnace for about 1hr to remove thermal strains that

are produced due to sudden quenching. The glasses thus obtained were highly grounded to achieve a uniform thickness of 0.2 cm.

Table 3.1. LTT glass composition with different concentrations of Pr^{3+} ions (mol %)

Name of the glass	TeO_2	WO_3	PbF_2	Pr_6O_{11}
Base Glass	60	25	15	---
LTTPr001	59.99	25	15	0.01
LTTPr01	59.9	25	15	0.1
LTTPr05	59.5	25	15	0.5
LTTPr10	59	25	15	1
LTTPr15	58.5	25	15	1.5

3.2.2 Physical and Optical Measurements

The famous Archimedes's principle is used to measure the densities for the prepared glasses with xylene as an immersion liquid. The refractive indices of all glasses were measured by using Brewster's angle method with He-Ne laser operating at 632 nm. Using density and refractive indices, some other physical properties [90] were also calculated using relevant equations (2.1-2.11) that are given in chapter-2 and are given in Table 3.2.

Table 3.2. Various physical properties of Pr^{3+} doped LTT glasses.

Physical properties	**LTTPr001**	**LTTPr01**	**LTTPr05**	**LTTPr10**	**LTTPr15**
Density ρ(g cm^{-3})	6.606	6.607	6.612	6.616	6.622
Refractive index(n_d)	2.305	2.306	2.307	2.308	2.309
Average molecular weight $\bar{M}$(g)	135.1	135.2	135.9	136.8	137.6
Pr^{3+}Ion contribution N(x10^{21} ions/cm^3)	0.294	2.941	14.643	29.122	43.451
Mean atomic volume(g/cm^3/atom)	6.629	6.296	6.308	6.324	6.338
Dielectric constant(**ε**)	5.315	5.320	5.325	5.329	5.334
Optical dielectric constant(ε-1)	4.315	4.320	4.325	4.330	4.334
Reflections loss(R %)	0.155	0.156	0.156	0.156	0.156
Molar refraction(R_m)(cm^{-3})	13.97	13.99	14.06	14.14	14.22
Polaron radius(Å)	0.210	0.066	0.029	0.021	0.017
Inter ionic distance(Å)	15.034	6.981	4.088	3.251	2.845
Molecular electronic Polarizability, α(x$10^{-23}$$cm^3$)	137.5	13.76	2.762	1.388	0.930
Field strength(x10^{22})	0.675	6.744	33.57	66.77	99.63
Optical basicity (Λ_{th})	0.540	0.541	0.542	0.544	0.545

In the present study the physical properties are changing from glass to glass with increase in the concentration of Pr^{3+} ions, indicating the change in environment around the doped Pr^{3+} ions. The optical absorption spectra were measured for all the glass samples from 440 to 2400 nm at room temperature with a spectral resolution of 0.1nm using Jasco V-670 UV-vis-NIR spectrometer. The luminescence spectra were measured by using PL spectrometer Perkin–Elmer LS55 with xenon arc lamp as radiation source.

3.3. Results and Discussion

3.3.1. Optical Absorption Spectra

Optical absorption spectra of Pr^{3+} ions doped LTT glasses were recorded at room temperature in vis-NIR region. Fig.3.1 shows the optical absorption spectra recorded for LTTPr10 along with the assignment of the absorption bands. The spectra for other glasses are alike with slender difference in intensity of various absorption bands and hence spectra of the remaining glasses were not shown. The band assignments are in good agreement with earlier reporters [103, 104].

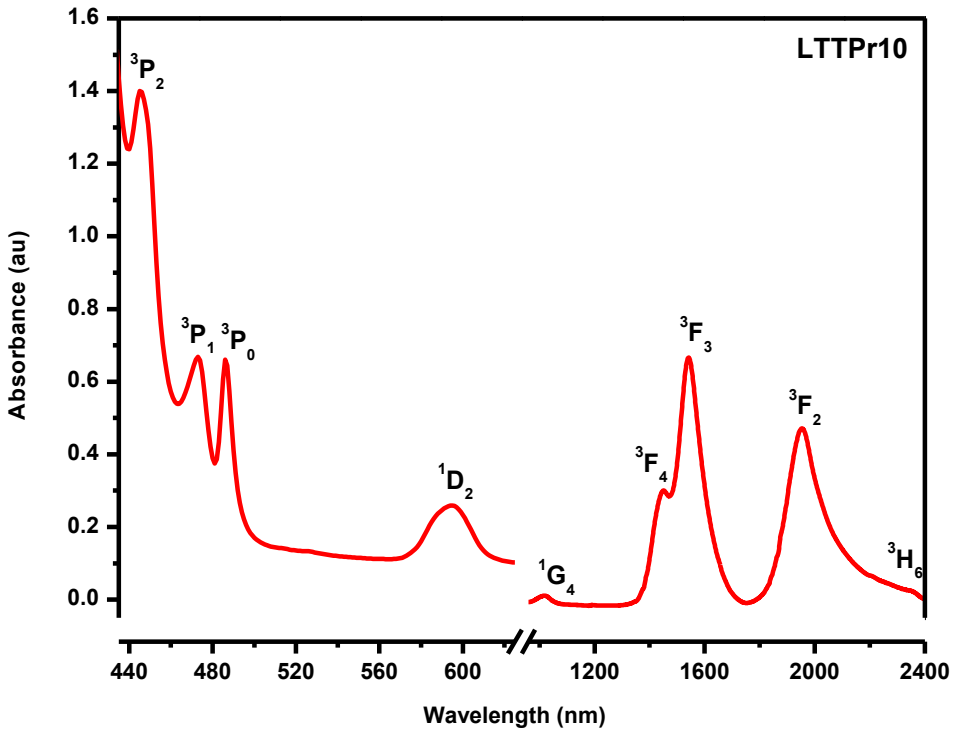

Fig. 3.1. Absorption spectrum of 1mol% of Pr^{3+} ions in LTT glass (LTTPr10) with strong absorption bands in the NIR region

Pr^{3+} ion doped LTT glasses contains nine absorption bands (except LTTPr001) corresponding to the transitions between the $^3H_4$ ground level and the excited states $^3P_2$, $^3P_1$, $^3P_0$, $^1D_2$,$^1G_4$, $^3F_4$, $^3F_3$,$^3F_2$ and $^3H_6$ belongs to the $4f^2$ configuration of the Pr^{3+} ions. The absorption bands are assigned to different transitions according to the Carnal report [105] on Pr^{3+} ion and the corresponding peak wavelength are given in Table 3.3. In LTTPr001, six absorption bands are only observed in vis-NIR regions may be due to very low concentration of Pr^{3+} ions (0.01 mol %) in that glass.

The experimental oscillator strengths (f_{exp}) for the electric dipole transitions have been determined [56] using the eq. (1.8) and such oscillator strengths for all the glasses are given in Table 3.3. In the present work, for all the absorption bands, the intensities were measured by area method. Of all the transitions, the transitions $^3H_4 \rightarrow {}^3P_2$ and $^3H_4 \rightarrow {}^3F_3$ are known as hypersensitive transitions whose intensities are strongly depends on the neighboring ligands [106].

Table 3.3. Assignment of absorption bands, experimental (f_{exp}) (10^{-6}), calculated oscillator strengths (f_{cal}) (10^{-6}) and r.m.s deviation (δ_{rms}) (10^{-6}) of Pr^{3+} ions doped LTT glasses using standard and modified J-O theories

Transition from $^3H_4 \rightarrow$	**λ (nm)**	**LTTPr001**			**LTTPr01**			**LTTPr05**			**LTTPr10**			**LTTPr15**		
		f_{exp}	**f_{cal}**	**f^*_{cal}**	**f_{exp}**	**f_{cal}**	**f^*_{cal}**	**f_{exp}**	**f_{cal}**	**f^*_{cal}**	**f_{exp}**	**f_{cal}**	**f^*_{cal}**	**f_{exp}**	**f_{cal}**	**f^*_{cal}**
$^3P_2$	445	-	-	-	-	-	-	6.49	5.61	7.45	8.87	6.06	8.80	6.33	4.70	6.26
$^3P_1$	473	-	-	-	5.37	8.03	7.66	4.59	6.34	6.33	7.31	7.54	7.67	5.11	6.19	6.27
$^3P_0$	486	-	-	-	2.02	7.91	7.47	3.79	6.25	6.18	4.32	7.42	7.49	4.13	6.10	6.12
$^1D_2$	596	1.26	1.20	1.47	2.30	1.56	1.91	3.62	1.88	2.27	3.92	2.04	2.47	3.09	1.55	1.88
$^1G_4$	1024	0.62	0.33	0.35	1.12	0.43	0.47	1.02	0.53	0.57	1.25	0.57	0.62	1.04	0.43	0.47
$^3F_4$	1453	3.16	3.17	3.17	1.37	4.21	4.70	4.16	5.76	6.05	4.69	6.12	6.46	3.31	4.59	4.87
$^3F_3$	1541	8.05	8.05	8.05	12.4	10.5	10.1	12.7	11.9	11.5	13.6	13.0	12.7	10.4	9.89	9.61
$^3F_2$	1956	8.36	8.35	8.35	14.2	14.3	14.3	15.1	15.1	15.1	16.7	16.7	16.7	11.1	11.11	11.1
$^3H_6$	2357	0.73	0.71	0.67	0.70	0.88	0.86	1.62	1.12	1.07	1.82	1.21	1.16	1.58	0.93	0.89
δ_{rms}		±0.11		±0.13	±2.61		±2.54	±1.35		±1.36	±1.64		±1.40	±1.19		±1.08

f_{cal} – calculated oscillator strengths from standard J-O theory

f^*_{cal} – calculated oscillator strengths from modified J-O theory

The hypersensitive transitions are observed in other RE ions and exhibit anomalous nature irrespective of matrix elements and follows selection rules $\Delta S = 0$, $\Delta L \leq 2$ and $\Delta J \leq 2$. Both Judd and Ofelt have derived expressions independently useful for the measurement of oscillator strengths of induced electric dipole transitions for the f^N configurations [47, 48].

The basic idea of the Judd-Ofelt (J-O) theory is that the intensity of the forbidden f-f electric dipole transitions can arise from the admixture of the $4f^N$ configurations with the excited configurations of opposite parity. The calculated oscillator strengths (f_{cal}) of the $\psi_J \rightarrow \psi'_{J'}$ transition are determined by using the relative expression given in chapter-1, using eq. (1.5) in the J-O theory [47, 48].

It is a well known fact that, the application of J-O theory to the 4f transitions of Pr^{3+} ion gives in poor agreement between the theoretical and experimental oscillator strengths [107-110]. This poor agreement between experimental and calculated oscillator strengths is expected because of small energy difference between $4f^2$ and 4f 5d levels. By applying modified J-O theory, it is possible to get reasonably good agreement between theoretical and experimental oscillator strengths with less r.m.s deviation including hypersensitive transition [111].

According to modified J-O theory, the experimental oscillator strengths (f_{exp}) for electric dipole transitions were calculated using the following expression.

$$f_{exp} = \frac{8\pi^2 mc\vartheta}{3h(2J+1)} \frac{(n^2+2)^2}{9n} \sum_{\lambda=2,4,6} \Omega_\lambda [1 + 2\alpha(E_J + E_{J'} - 2E_{f^0})] \left(\psi_J \| U^\lambda \| \psi'_{J'}\right)^2 \quad (3.1)$$

Here E_J is the energy of the ground state, $E_{J'}$ is the energy of excited state, E_{f^0} energy of the center of gravity of the $4f^2$ configuration (~ 10,000 cm^{-1}) and $\alpha = \frac{1}{2}[E(4f5d) - E(4f)$. The parameter α has a value of 10^{-5} cm^{-1}, but in practice it is treated as an additional fitting parameter. The calculated oscillator strengths measured by using standard as well as modified J-O theories including $^3H_4 \rightarrow {}^3P_2$ hypersensitive transition are tabulated in Table 3.3 along with the experimental oscillator strengths. From Table 3.3 it is observed that, for most of the LTT glasses, the modified J-O theory gives good approximation between experimental and calculated oscillator strengths with less r.m.s deviation than standard J-O theory. Table 3.4 gives J-O parameters measured for all the LTT glasses using standard and modified J-O theories along with their trend. Significant improvement in J-O intensity parameters can be observed after applying the modified

J-O theory. Except for LTTPr001, the trend followed by J-O intensity parameters is same ($\Omega_2>\Omega_4>\Omega_6$) for all LTT glasses in both standard as well as modified J-O theories. From both the J-O theories, the Ω_2 parameter is found to be maximum for all the LTT glasses.

Table 3.4. Judd-Ofelt intensity parameters Ω_2, Ω_4 and Ω_6 (10^{-20} cm^2) and their trend for Pr^{3+} doped LTT glasses with Standard and modified J-O theories

Name of the glass sample	Standard J-O Theory			Trend followed in Standard J-O theory	Modified J-O Theory*			Trend followed in Modified J-O theory
	Ω_2	Ω_4	Ω_6		Ω_2^*	Ω_4^*	Ω_6^*	
LTTPr001	4.782	6.148	2.208	$\Omega_4> \Omega_2> \Omega_6$	5.402*	6.609*	2.318*	$\Omega_4> \Omega_2> \Omega_6$
LTTPr01	11.06	7.156	2.854	$\Omega_2> \Omega_4> \Omega_6$	13.90*	5.557*	3.641*	$\Omega_2> \Omega_4> \Omega_6$
LTTPr05	12.88	5.648	4.412	$\Omega_2> \Omega_4> \Omega_6$	15.43*	4.590*	5.041*	$\Omega_2> \Omega_6> \Omega_4$
LTTPr10	13.89	6.70	4.606	$\Omega_2> \Omega_4> \Omega_6$	16.69*	5.559*	5.305*	$\Omega_2> \Omega_4> \Omega_6$
LTTPr15	8.309	5.503	3.481	$\Omega_2> \Omega_4> \Omega_6$	10.30*	4.542*	4.045*	$\Omega_2> \Omega_4> \Omega_6$

It is a known fact that, the physical property such as viscosity and the chemical property such as covalent nature of chemical bonds relates to the magnitudes of J-O intensity parameters. In general, the Ω_2 J-O parameter values are intermediate between crystalline oxides and chelating ligands [112-114]. Rare earth ions in glasses, are randomly distributed over non-equivalent sites with a wide distribution of crystal fields. As a result, a distribution of large number of rare earth ions occupying sites with non-centrometric potential will contribute significantly to the changes in the Ω_2 J-O value [115]. The Ω_2 J-O parameter value is directly proportional to the covalent character of the chemical bonds among the glass matrix and rare earth ions. The asymmetry of the sites around the rare earth ion influences the Ω_2 J-O parameter. The higher the Ω_2 parameter, the higher is the degree of asymmetry around the rare earth ion and stronger the covalence of rare earth ion-oxygen bond. The bulk properties of the material medium such as viscosity and dielectric constants depend on the JO parameters Ω_4 and Ω_6. They are also influenced by the vibronic transitions of the rare earth ions bound to the ligand atoms [116, 117]. However they are less sensitive to the medium in which the ions are situated. From Table 3.4, it is observed that, the J-O intensity parameters are found to be high for LTTPr10, indicating that it is more asymmetric, more covalent and more rigid than the other LTT glasses.

3.3.2. Photoluminescence Properties

To analyze the photoluminescence properties of the LTT glasses doped with Pr^{3+} ion, it is necessary to know the excitation wavelength of Pr^{3+} ion. The excitation wavelength plays an important role in recording the emission spectra of rare-earth ions doped luminescent materials. Fig. 3.2 shows the excitation spectra of LTTPr10 when emission is monitored at 644 nm.

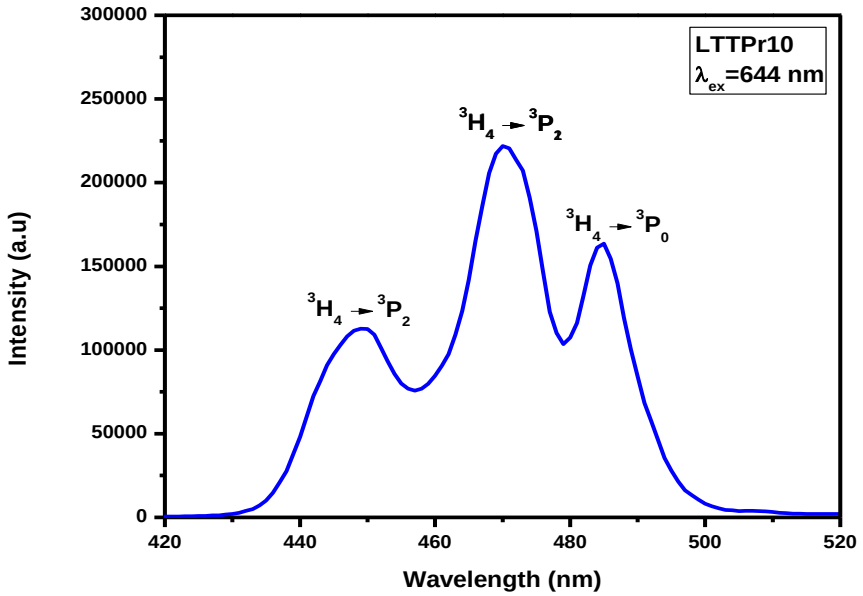

Fig. 3.2. Excitation spectrum of 1mol% of Pr^{3+} ions in LTT glass (LTTPr10)

The excitation spectra consist of three bands corresponding to the transitions $^3H_4 \rightarrow {}^3P_2$, $^3H_4 \rightarrow {}^3P_1$ and $^3H_4 \rightarrow {}^3P_0$. Among all these transitions, a transition observed at 470 nm and pertaining to $^3H_4 \rightarrow {}^3P_1$ transition is more intense and is used as an excitation wavelength to record the emission spectra. The emission spectra recorded at room temperature for LTT glasses doped with different concentration of Pr^{3+} ions in the spectral range 550-750 nm are shown in Fig.3.3.

The emission spectra consist of five emission bands at 613, 644, 683, 707 and 730 nm corresponding transitions to $^3P_0 \rightarrow {}^3H_6$, $^3P_0 \rightarrow {}^3F_2$, $^3P_1 \rightarrow {}^3F_3$, $^3P_1 \rightarrow {}^3F_4$ and $^3P_0 \rightarrow {}^3F_4$ respectively. Fluorescence quenching is observed in all the emission transitions with

increase in the concentration of Pr^{3+} ions. The quenching of intensity is same for all the emission transitions except for $^3P_0 \rightarrow {}^3H_6$ transition. Fluorescence quenching for all the emission transitions begins at 1.0 mol % but for $^3P_0 \rightarrow {}^3H_6$ transition, the quenching began at 0.1mol % of Pr^{3+} ion concentration itself. This may be due to the energy transfer through cross-relaxation between Pr^{3+} ions. Fig.3.3 also shows that, with increase in Pr^{3+} ion concentration, a significant red shift has been observed for $^3P_0 \rightarrow {}^3H_6$ emission transition.

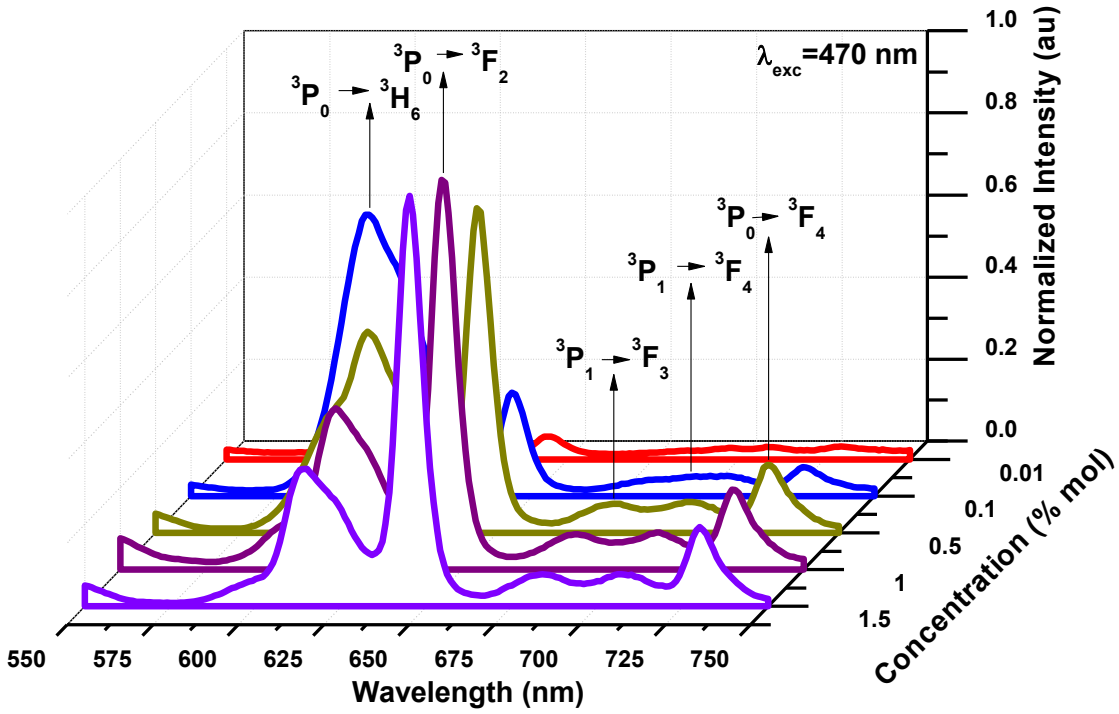

Fig. 3.3. Emission spectra of Pr^{3+} ions in LTT glasses

The peak position of $^3P_0 \rightarrow {}^3H_6$ transition in LTT glasses observed at 600, 602, 611, 613 and 614 nm for 0.01, 0.1, 0.5, 1.0 and 1.5 mol% of Pr^{3+} ion concentration respectively indicates a red shift of the that peak. In the vicinity of ligand field the site distribution of Pr^{3+} ions may cause the red shift [118]. However, no red shift was observed for the other transitions namely $^3P_0 \rightarrow {}^3F_2$, $^3P_1 \rightarrow {}^3F_3$, $^3P_0 \rightarrow {}^3F_3$ and $^3P_0 \rightarrow {}^3F_4$ because of negligible emission intensities of the respective emission bands. Fig.3.4 represents the energy level diagram depicting the various lasing transitions for 1 mol % of pr^{3+} ions in LTT glass (LTTPr10). From Fig.3.4, it is

observed that the emission occurs only from $^3P_0$, which indicates that $^3P_1$ state is thermally populated.

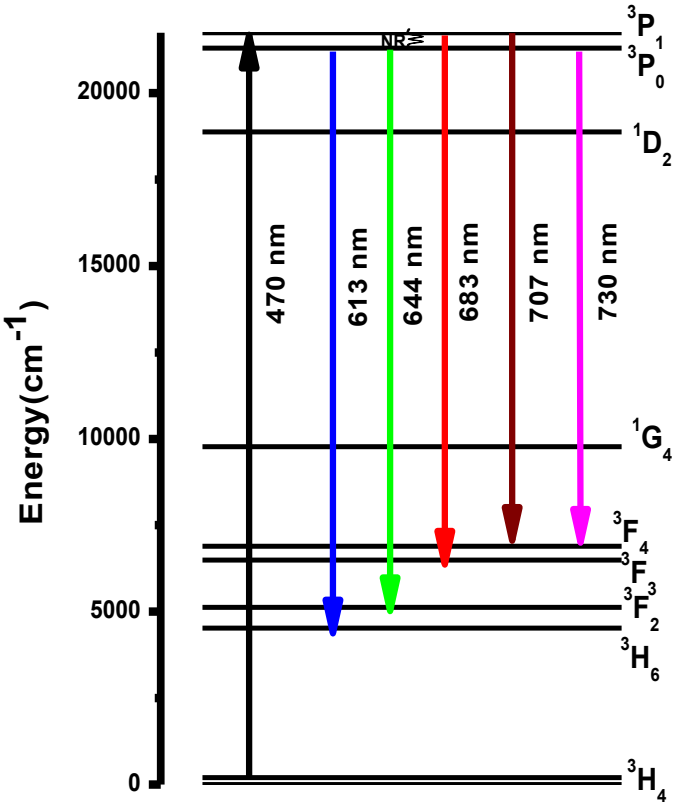

Fig. 3.4. Energy level scheme for emission process of 1mol% Pr^{3+}ions in LTT glass (LTTPr10)

In order to predict the emission performance of LTT glasses doped with Pr^{3+} ions, the radiative parameters such as radiative transition probability (A_R), total radiative transition probability (A_T), radiative lifetime (τ_R), branching ratio (β_R) and stimulated emission cross-section (σ_{se}) were measured for the observed fluorescent levels using J-O parameters derived from modified J-O theory. The necessary mathematical expressions needed to measure the above radiative parameters eq. (1.10-1.13) were given in chapter-1. The radiative parameters thus evaluated are given in Tables [3.5 to 3.7]. In addition to these parameters, the other radiative parameters like gain band width ($\sigma_{se} \times \Delta\lambda_P$) and optical gain parameters ($\sigma_{se} \times \tau_R$), which are also important to identify a laser active medium are evaluated and included in Table 3.7.

Table 3.5 gives the transition probability (A_R), total transition probability (A_T) and radiative lifetimes (τ_R) for the observed emission transitions of Pr^{3+} ions doped LTT glasses. Large transition probability value obtained for LTTPr10 for $^3P_1 \rightarrow {}^3F_3$ fluorescent level speaks the potentiality of LTTPr10 over the other LTT glasses.

Table 3.6 represents the measured and experimental branching ratios (β_R) observed for all the emission transitions of Pr^{3+} doped LTT glasses. The emission transitions with higher magnitude of β_R are more competent for laser action than the other transitions originating from a given excited state. From Table 3.6, it can be observed that β_R value for $^3P_0 \rightarrow {}^3F_2$ transition is more than the other transitions in all LTT glasses. This speaks the potentiality of this energy level for laser emission at 644 nm in these LTT glasses. From 3.6, it can also be observed that the β_R and β_{exp} are in good agreements with each other for all the transitions in LTT glasses. Table 3.7 gives the emission peak wavelength (λ_P), effective band widths ($\Delta\lambda_P$), stimulated emission cross-sections (σ_{se}), gain band width ($\sigma_{se} \times \Delta\lambda_P$) and optical gain parameter ($\sigma_{se} \times \tau R$) for the emission transitions of Pr^{3+} ions doped LTT glasses. Stimulated emission cross-section have been evaluated using eq. (1.14), which signifies the energy extraction for the material is an important parameter to estimate laser performance of a material. From Table 3.7, it is observed that among all the emission transitions, $^3P_0 \rightarrow {}^3F_2$ (644nm) and $^3P_0 \rightarrow {}^3H_6$ (602 nm) transitions possess highest and least stimulated emission cross-sections respectively.

This may be due to the variation of in-homogenous line widths of the two transitions. In the present LTT glasses, the LTTPr10 with 1 mol % of Pr^{3+} ions possess highest stimulated emission cross-section for all the transitions. In LTTPr10, $^3P_0 \rightarrow {}^3F_2$ transition (644 nm) possess highest stimulated emission cross-section over the other transitions in the same glass. Hence LTTPr10 is said to be having enough competency to emit bright red laser at 644 nm. The gain parameters ($\sigma_e x \tau_m$) and gain band width ($\sigma_e x \Delta\lambda_p$) are used to obtain a laser host material with highest stability [119].

In the present work, the gain properties of $^3P_0 \rightarrow {}^3F_2$ level are found to be maximum for all the LTT glasses. Among all the glasses, LTTPR10 possesses higher values of these parameters. Based on the measured radiative parameters, it is suggested that LTTPr10 doped with 1mol % of Pr^{3+} ions can be used for red laser emission at 644

nm corresponding to the transitions $^3P_0 \rightarrow ^3F_2$ and it is also useful for optical amplification.

Table 3.5.

Transition probabilities (A_R) (s^{-1}), total transition probability (A_T) (s^{-1}) and radiative lifetimes (τ_R) (μs) for the observed prominent emission transitions of Pr^{3+} doped LTT glasses.

Transition	LTTPr001			LTTPr01			LTTPr05			LTTPr10			LTTPr15		
	A_R	A_T	τ_R	A_R	A_T	τ_R	A_R	A_T	τ_R	A_R	A_T	τ_R	A_R	A_T	τ_R
$^3P_1 \rightarrow {}^3F_4$	16914	175196	5	14294	245767	4	11787	249880	4	14300	280367	3	11703	195693	5
$^3P_1 \rightarrow {}^3F_3$	45984	175196	5	94941	245767	4	102262	249880	4	112030	280367	3	71559	195693	5
$^3P_0 \rightarrow {}^3F_4$	18598	190419	5	15720	269284	3	12960	272646	3	15723	306094	3	12868	212646	4
$^3P_0 \rightarrow {}^3F_2$	59343	190419	5	152956	269284	3	170080	272646	3	184281	306094	3	113919	212646	4
$^3P_0 \rightarrow {}^3H_6$	7492	190419	5	11788	269284	3	16348	272646	3	17234	306094	3	13163	212646	4

Table 3.6.

Measured (β_R) and experimental (β_{exp}) branching ratios of different concentrations of Pr^{3+} ions doped LTT Glasses.

Transition	LTTPr001		LTTPr01		LTTPr05		LTTPr10		LTTPr15	
	β_R	β_{exp}	β_R	β_{exp}	β_R	β_{exp}	β_R	β_{exp}	β_R	β_{exp}
$^3P_1 \rightarrow {}^3F_4$	0.096	0.050	0.058	0.283	0.047	0.315	0.051	0.050	0.059	0.032
$^3P_1 \rightarrow {}^3F_3$	0.262	0.191	0.386	0.109	0.409	0.304	0.399	0.409	0.365	0.456
$^3P_0 \rightarrow {}^3F_4$	0.097	0.044	0.058	0.034	0.047	0.052	0.051	0.062	0.060	0.067
$^3P_0 \rightarrow {}^3F_2$	0.311	0.146	0.568	0.231	0.623	0.248	0.602	0.166	0.535	0.103
$^3P_0 \rightarrow {}^3H_6$	0.039	0.067	0.043	0.042	0.060	0.080	0.056	0.112	0.061	0.012

Table 3.7.
Emission peak wavelength (λ_P)(nm), effective band widths($\Delta\lambda_P$)(nm), stimulated emission cross-sections (σ_{se}) ($x10^{-20}$) (cm^2), gain band width (σ_{se} x $\Delta\lambda_p$) (10^{-25}) (cm^3) and optical gain parameters (σ_{se} x τ_R) (10^{-25}) (cm^2 s) for the emission transitions of Pr^{3+} doped LTT glasses

Spectral parameters	LTTPr001	LTTPr01	LTTPr05	LTTPr10	LTTPr15
$^3P_0 \rightarrow {}^3H_6$					
λp	600	602	611	613	614
$\Delta\lambda p$	16.3	8.11	12.0	13.0	16.3
σ_{se}	1.49	4.76	4.73	4.66	2.83
σ_{se} x $\Delta\lambda p$	0.24	0.38	0.56	0.60	0.46
σ_{se} x τ_R	0.74	1.43	1.42	1.40	1.14
$^3P_0 \rightarrow {}^3F_2$					
λp	644	644	644	644	644
$\Delta\lambda p$	7.61	6.52	5.43	4.89	5.43
σ_{se}	33.5	101.0	134.0	161.0	89.8
σ_{se} x $\Delta\lambda p$	2.55	6.57	7.29	7.90	4.88
σ_{se} x τ_R	16.8	30.2	40.3	48.4	35.9
$^3P_1 \rightarrow {}^3F_3$					
λp	683	683	683	683	683
$\Delta\lambda p$	8.11	6.76	9.46	4.05	9.46
σ_{se}	30.8	76.3	58.7	150.0	41.0
σ_{se} x $\Delta\lambda p$	2.50	5.16	5.55	6.07	3.88
σ_{se} x τ_R	15.4	30.5	23.5	45.0	20.5
$^3P_1 \rightarrow {}^3F_4$					
λp	707	707	707	707	707
$\Delta\lambda p$	14.9	13.5	12.5	12.2	13.5
σ_{se}	7.08	6.60	5.87	7.30	5.39
σ_{se} x $\Delta\lambda p$	1.06	0.89	0.73	0.89	0.72
σ_{se} x τ_R	3.54	2.64	2.35	2.19	2.70
$^3P_0 \rightarrow {}^3F_4$					
λp	730	730	730	730	730
$\Delta\lambda p$	9.46	10.8	8.11	6.76	8.11
σ_{se}	13.9	10.3	11.3	16.5	11.2
σ_{se} x $\Delta\lambda p$	1.32	1.11	0.91	1.11	0.91
σ_{se} x τ_R	6.97	3.09	3.39	4.94	4.49

3.3.3 CIE Chromaticity Co-ordinates

The CIE coordinates are used to find the color of the light emitted by the material under excitation. They are measured from the emission spectra given by the materials under investigation. Such CIE co-ordinate measured from the emission spectra of LTT glasses doped with Pr^{3+} ions using the CIE system are presented in Table 3.8. The emission spectra contain three parts. The first part is orange to red, second part is

red and the third part is NIR. The CIE color co-ordinates for all the samples are evaluated from the emission spectra following the procedure outlined in the commission International de I'Eclaiage France CIE system using eq. (1.21-1.25) and are found to be in the bright red region. Among all the glass samples, particularly LTTPr10 color co-ordinates (x=0.65, y=0.27) are falling in the bright red region corresponding to $^3P_0 \rightarrow {}^3F_2$ (644 nm) transition. Fig. 3.5 represents the CIE plot with color co-ordinates for 1mol% of Pr^{3+} in LTT glass (LTTPr10) excited at 470 nm wavelength. Hence LTTPr10 is with 1 mol% of Pr^{3+} ions are quite suitable to give bright red color laser at 644 nm.

Table 3.8.

CIE chromaticity co-ordinates of Pr^{3+} ions doped LTT glasses

Name of the glass	Colour Co-ordinates	
	X-Co-ordinates	Y-Co-ordinates
LTTPr001	0.6343	0.3564
LTTPr01	0.6423	0.3523
LTTPr05	0.6646	0.3345
LTTPr10	0.6512	0.2785
LTTPr15	0.6435	0.2764

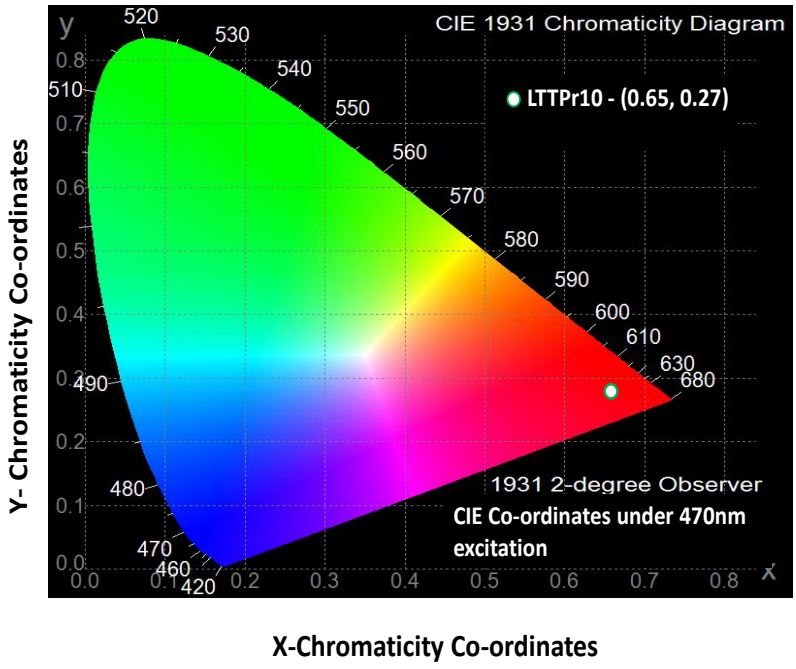

Fig. 3.5. CIE 1931 chromaticity diagram for 1mol% of Pr^{3+} ions in LTT glass (LTTPr10)

3.4. Conclusion

Lead Tungsten Tellurite **(**LTT) glasses doped with different concentrations of Pr^{3+} ions were prepared by using conventional melt quenching technique. The amorphous nature of the prepared LTT glasses were confirmed by XRD spectrum recorded for an undoped LTT glass. The modified J-O theory has been applied to analyze the absorption spectra of Pr^{3+} ions doped LTT glasses. The J-O intensity parameters calculated by using the modified J-O theory give less r.m.s deviation between experimental and calculated oscillator strengths. In the present work, the J-O intensity parameters (Ω_2, Ω_4 and Ω_6) are found to be high for LTTPr10 indicating that it is more asymmetric, more covalent and more rigid than the other glasses. Using the J-O parameters obtained from the modified J-O theory, the radiative properties such as transition probability (A_R), radiative lifetime (τ_R) and branching ratios (β_R) are evaluated. The emission spectra recorded at different concentrations of Pr^{3+} ions show five emission bands at 613, 644, 683, 707 and 730 nm corresponding transitions to $^3P_0 \rightarrow {}^3H_6$, $^3P_0 \rightarrow {}^3F_2$, $^3P_1 \rightarrow {}^3F_3$, $^3P_1 \rightarrow {}^3F_4$ and $^3P_0 \rightarrow {}^3F_4$ respectively. Among these five emission transitions observed, $^3P_0 \rightarrow {}^3F_2$ is more intense and is falling in red region. Based on visible emission spectra, the high stimulated emission cross-section and branching ratios observed for $^3P_0 \rightarrow {}^3F_2$ transition for all these glasses suggest the feasibility of using these materials as lasers in red region. The CIE chromaticity co-ordinates evaluated from the emission spectra recorded at 470 nm excitation for all LTT glasses confirms the suitability of these glassy materials for red emission. From the measured emission cross-sections and CIE chromaticity co-ordinates, it was found that 1mol% of Pr^{3+} ions in LTT glasses (LTTPr10) is aptly suitable for the development of bright visible red lasers to operate at 644 nm from these LTT glasses.